

# NUMERICAL ANALYSIS OF NATURAL CONVECTION INSIDE THE BUILDING

**Gilberto Augusto Amado Moreira, gilbertomoreira@ufmg.br**

**Rudolf Huebner, rudolf@demec.ufmg.br**

**Ramón Molina Valle, ramon@demec.ufmg.br**

Universidade Federal de Minas Gerais (UFMG). Av. Antônio Carlos, 6627 - Pampulha - Belo Horizonte – MG, CEP 31270-901.

**Abstract.** *Natural ventilation inside constructions allows both favorable conditions for thermal comfort to the occupants and quality improvement of the internal air. The efficiency of natural ventilation in a building is associated to the number, position, type and size of the existing openings for the passage of air. It is also associated to the combined action of wind forces and temperature differences. Thus the construction of openings in both the front and in the coverage of buildings, provide improvements in natural ventilation also assisting in the internal lighting environments. This paper aims to analyze numerically the natural ventilation within an industrial shed. This will be used for a commercial software which solves the equations governing this type of flow in their conservative (the conservation of mass equation, momentum and energy) coupled to a turbulence model. The results will be compared with analytical methodologies for analysis of the use openings in the roofs (skylight with an entrance and an exit) in sheds and natural convection, validated methodology that provides a better analysis of thermo-fluid dynamics processes within buildings.*

**Keywords:** *Thermo-fluid dynamics processes; Natural convection; CFD*

## 1. INTRODUCTION

The Natural ventilation inside constructions allows both favorable conditions for thermal comfort to the occupants and quality improvement of the internal air. The efficiency of natural ventilation in a building is associated to the number, position, type and size of the existing openings for the passage of air. It is also associated to the combined action of wind forces and temperature differences. Thus the construction of openings in both the front and in the coverage of buildings, provide improvements in natural ventilation also assisting in the internal lighting environments.

In the past two decades, building fire field model (or application of computational fluid dynamics (CFD)) has been developed and used to some extent in the construction industry for fire designs and related academic research projects.

The study of natural convection through mathematical techniques were demonstrated by several researchers, where we cite a few works such as Chow (1996) who conducted a study showing the importance of CFD techniques to the behavior of various phenomena (fire, air conditioning, heat distribution, among others) inside buildings, experimentally validating their various cases. Likewise, Mazon (2006) and Ji (2007) also through Computational Fluid Dynamics also demonstrated the efficiency of this methodology in predicting the flow of natural convection.

Macintyre (1990), Costa (2005) among other authors conservative formulations have to scale buildings as well as the use of CFD in this work is expected to be a better approximation to the real data.

The objective of this work is to study through computational fluid dynamics (CFD) is possible to predict the fluid dynamic behavior of the heated air inside buildings, making sure that the formulations presented by Marc are consistent in size, openings for air exchanges between the interior and exterior of buildings and thereby ensure the thermal comfort inside.

## 2. METHODOLOGY

The modeling and the simulation of the flow are made using the commercial package Ansys CFX-11.0, “CFX (2004)”. This software possesses the following characteristics: discretize the conservation equations by the finite volumes method centered in the vertex; solves laminar and turbulent three-dimensional problems; uses unstructured and hybrid meshes; solves conjugated problems of heat and fluids flow. The use of no-structured meshes allows mesh refinements to be applied near the surfaces, where great variations of speed and temperature occur.

The Equations (1, 2 e 3) represent respectively, conservation of mass, momentum and energy, respectively, under the decomposition of Reynolds and Boussinesq approximation. The term  $S_M$  defined in Equation 2, represents the end of fluctuation.

$$\frac{\partial \rho}{\partial t} + \nabla \cdot (\rho U) = 0 \quad (1)$$

$$\frac{\partial (\rho U)}{\partial t} + \nabla \cdot (\rho U \otimes U) = -\nabla p + \nabla \cdot \tau + S_M \quad (2)$$

$$\frac{\partial(\rho e)}{\partial t} + \nabla \cdot (\rho U e) = -\nabla \cdot (pU) + \nabla \cdot (k\lambda T) + \Phi + S_i \quad (3)$$

$$p = p(\rho, T) \text{ and } i = i(\rho, T) \quad (4)$$

Where all the effects due to viscous stresses in the internal energy equation are describe by dissipation function  $\Phi$ , which, after considerable algebra, can be shown to equal to:

$$\Phi = \mu \left\{ 2 \left[ \left( \frac{\partial u}{\partial x} \right)^2 + \left( \frac{\partial v}{\partial y} \right)^2 + \left( \frac{\partial w}{\partial z} \right)^2 \right] + \left( \frac{\partial u}{\partial y} + \frac{\partial v}{\partial x} \right)^2 + \left( \frac{\partial u}{\partial z} + \frac{\partial v}{\partial x} \right)^2 + \left( \frac{\partial v}{\partial z} + \frac{\partial w}{\partial y} \right)^2 \right\} + \nabla \cdot (\rho U) \quad (5)$$

The source term showed in Equation (2) is used for Buoyancy Forces, can be shown to equal to

$$S_M = (\rho - \rho_{ref})g \quad (6)$$

## 2.1 Turbulence Model

The model of turbulence quite robust and capable of predicting this flow is the SST-k-RNG k- $\omega$ , which uses the turbulent viscosity ( $\mu_t$ ), together with the equations of transport of the turbulent kinetic energy,  $k$ , and the dissipation of energy,  $\epsilon$ , where these terms are defined by CFX (2004) as:

### 2.1.1 The k- $\omega$ models

The k- $\omega$  models assumes that the turbulence viscosity is linked to the turbulence kinetic energy and turbulent frequency via the relation:

$$\mu_t = \rho \frac{k}{\omega} \quad (7)$$

Where the k- $\omega$  model developed by Wilcox (1986) solves two transport equations, one for the turbulent kinetic energy,  $k$ , and one for the turbulent frequency,  $\omega$ . The stress tensor is computed from the eddy-viscosity concept.

k-equation:

$$\frac{\partial(\rho k)}{\partial t} + \nabla \cdot (\rho U k) = \nabla \cdot \left[ \left( \mu + \frac{\mu_t}{\sigma_k} \right) \nabla k \right] + P_k - \beta' \rho k \omega \quad (8)$$

$\omega$ -equation:

$$\frac{\partial(\rho \omega)}{\partial t} + \nabla \cdot (\rho U \omega) = \nabla \cdot \left[ \left( \mu + \frac{\mu_t}{\sigma_\omega} \right) \nabla \omega \right] + \alpha \frac{\omega}{k} P_k - \beta \rho k \omega^2 \quad (9)$$

In addition to the independent variables, the density,  $\rho$ , and the velocity vector,  $U$ , are treated as known quantities from the Navier-Stokes method.  $P_k$  is the production rate of turbulence.

The model constants are given by:

Table 1. The k- $\omega$  model constants

$\beta'$	$\alpha$	$\beta$	$\sigma_k$	$\sigma_\omega$
0.09	5/9	0.075	2	2

The unknown Reynolds stress tensor,  $\tau$ , is calculated from:

$$\tau = \mu_t 2s - \rho \frac{2}{3} \delta k \quad (10)$$

In order to avoid the build-up of turbulent kinetic energy in stagnation regions, two production limiters are available.

### 2.1.2 The Shear Stress Transport (SST)

The  $k-\omega$  based SST model accounts for the transport of the turbulent shear stress and gives highly accurate predictions of the onset and the amount of flow separation under adverse pressure gradients.

The BSL model combines the advantages of the Wilcox and the  $k-\varepsilon$  model, but still fails to properly predict the onset and amount of flow separation from smooth surfaces. The reasons for this deficiency are given in detail in Menter (1992). The main reason is that both models do not account for the transport of the turbulent shear stress. This results in an over prediction of the eddy-viscosity. The proper transport behavior can be obtained by a limiter to the formulation of the eddy-viscosity:

$$v_t = \frac{a_1 k}{\max(a_1 \varpi, SF_2)} \quad (11)$$

Where

$$v_t = \frac{\mu_t}{\rho} \quad (12)$$

Again  $F_2$  is a blending function similar to  $F_1$ , which restricts the limiter to the wall boundary layer, as the underlying assumptions are not correct for free shear flows.  $S$  is an invariant measure of the strain rate.

Blending Functions

The blending functions are critical to the success of the method. Their formulation is based on the distance to the nearest surface and on the flow variables.

$$F_1 = \tanh(\arg_1^4) \quad (13)$$

Whith:

$$\arg_1 = \min \left( \max \left( \frac{\sqrt{k}}{\beta' \omega y}, \frac{500v}{y^2 \omega} \right), \frac{4\rho k}{CD_{k\omega} \sigma_{\omega 2} y^2} \right) \quad (14)$$

Where  $y$  is the distance to the nearest wall,  $v$  is the kinematic viscosity and:

$$CD_{k\omega} = \max \left( 2\rho \frac{1}{\sigma_{\omega 2} \omega} \nabla k \nabla \omega, 1.0 \cdot 10^{-10} \right) \quad (15)$$

$$F_2 = \tanh(\arg_2^2) \quad (16)$$

With:

$$\arg_2 = \max \left( \frac{2\sqrt{k}}{\beta' \omega y}, \frac{500v}{y^2 \omega} \right) \quad (17)$$

### 2.2 Radiation Model

The simulation of heat exchange between the various surfaces by means of radiation was made using the method of Monte Carlo. In this case it was necessary to define the values of emissivity for each surface considered. Table 2 summarizes the values taken from literature Incropera and DeWitt (2003). If the emissivity of casting material was between the values presented by Seggiano (1988), Kreith (2003), Pirker at al. (2002) and Gosselin and Lacroix (2003).

Table 2. Emissivity Values

Location	Emissivity
Casting Material	0,7
Roof	0,92
Walls	0,92
Ground	0,93

### 2.3 Domain Computational

The Figure 1 (a) shows the computational domain used, where the side vents (red) represent the air inlet and the openings in the roof (green) are supposed to air exits. The blue areas designated by R1, R2, R3 and R4 represent plans to generate heat. The Figure 1 (b) study shows plans for the disposal sites (P1, P2, P3 and P4, shows that besides the dimensions of the shed ( $W = 30\text{ m}$ ,  $L = 70\text{ m}$   $H = 15\text{ m}$ ).

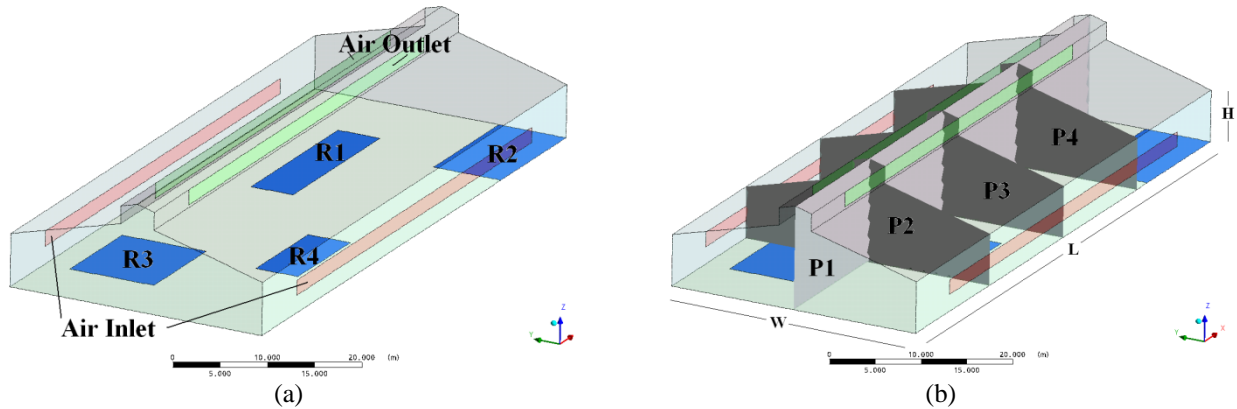


Figure 1. Boundary condition locations in the computational domain.

To represent a situation where involves a extreme case, external sources were not considered as wind and heat. Like this the Table 3 showed the boundary conditions imposed on the surfaces R1, R2, R3 and R4.

Table 3. Boundary conditions imposed on the surfaces R1, R2, R3 and R4

Region	Temperature (K)	Heat Load (kW)
R1	573,15	586,05
R2	673,15	951,91
R3	573,15	298,21
R4	673,15	1131,59

### 2.4 Mesh Study

To analyze the error made by the numerical model various configurations of meshes were used, well as they refine the error between a loop and another decreased. However some settings are necessary for the success of the study, as the influence of wall model in the turbulence model in the physics of the problem, besides more refined mesh near the wall and the hot sources to avoid propagation of errors in numerical analysis, limited by the wall model.

The Figure 2 (a) shows the mesh detail near the 3 plans P1 and P2 on the surface R3 and Figure 2 (b) also shows details of the plan P2 on the surface R3, showing the level of detail near the surface.

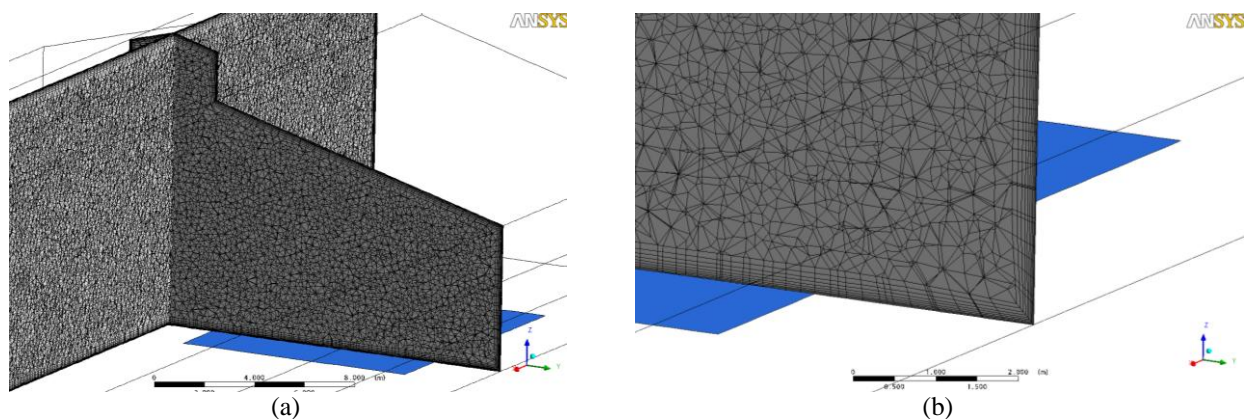


Figure 2. Mesh detail

The Table 4 shows details of the meshes used in numerical simulation showing the error found in each mesh used, showing the error found in each mesh used, besides the  $y_{plus}$ . The parameter  $y_+$  ( $y_{plus}$ ) is a non-dimensional variable based on the distance from the wall through the boundary layer to the first node away from the wall. It is therefore dependent on the size of the mesh in the wall region. If the alue of  $y_+$  is too large, then the wall function will impose wall type conditions further from the wall than would normally be physically appropriate. Well with this value of  $y_{plus}$  guarantees a good approximation near the wall, thus not compromising the results.

Table 4. Details of the meshes used in numerical simulation.

Mesh	Total Number of Nodes	Total Number of Elements	Error (%)	$Y_+$
1	419508	1538110		17,46
2	823897	3045947	14,5	17,76
3	1606401	6585645	3,9	20,05

### 3. RESULTS

The results shown in Figures 3 to 6, velocity vectors (a) and isosurfaces (b) at P1, P2, P3 and P4, as shown in Figures 7 velocity vectors in detail near the roof (a) and a hot source (b). In all Figures show upward acceleration of the flow due to heating of air masses, showing the ability of the model to represent the natural convection. The Table 5 shows the results of mass flow in entry and exit air regions. The negative sign represents the direction of flow in the computational domain (output).

Table 5. - Mass flow in entry and exit air regions.

Region	Mass Flow $m^3/h$
Air Inlet 1	83901,5
Air Inlet 2	77144,9
Air Outlet 1	-78157,7
Air Outlet 2	-82888,7

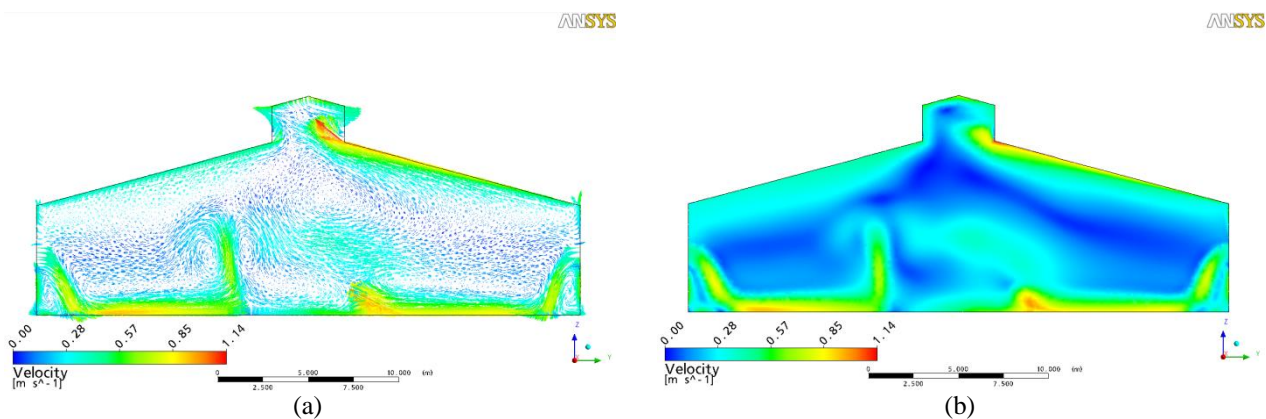


Figure 3. Velocity distribution on the region P1, velocity vectors (a) and velocity isosurfaces (b).

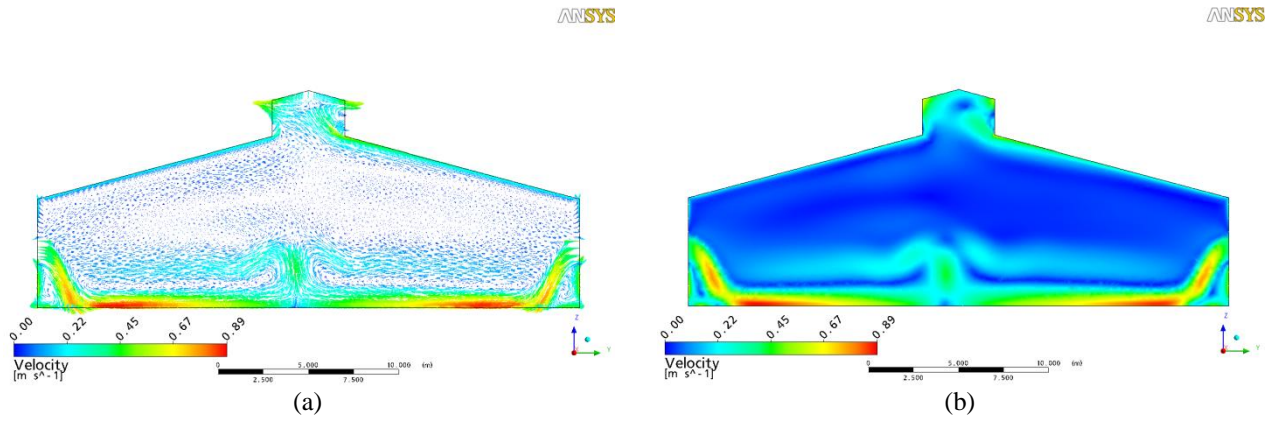


Figure 4. Velocity distribution on the region P2, velocity vectors (a) and velocity isosurfaces (b).

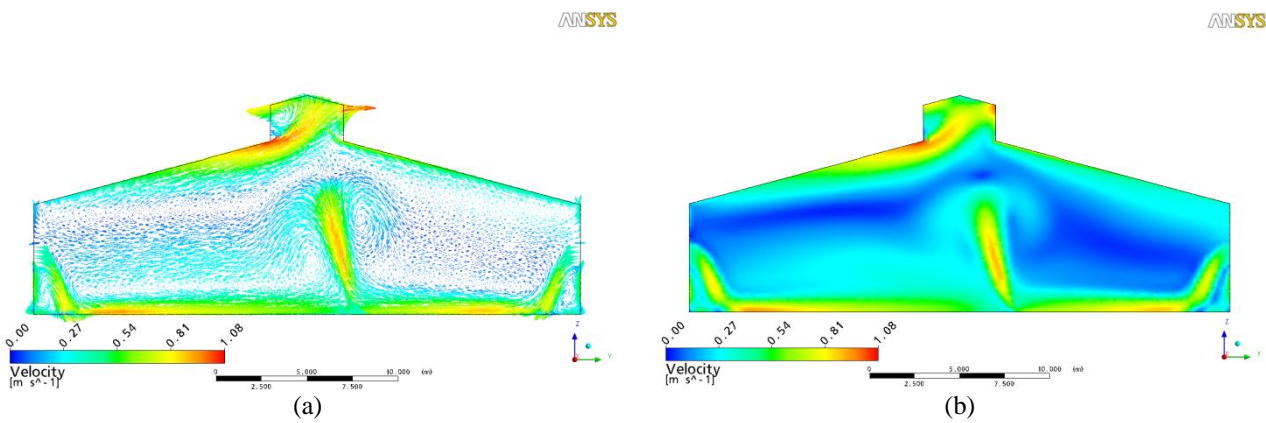


Figure 5. Velocity distribution on the region P3, velocity vectors (a) and velocity isosurfaces (b).

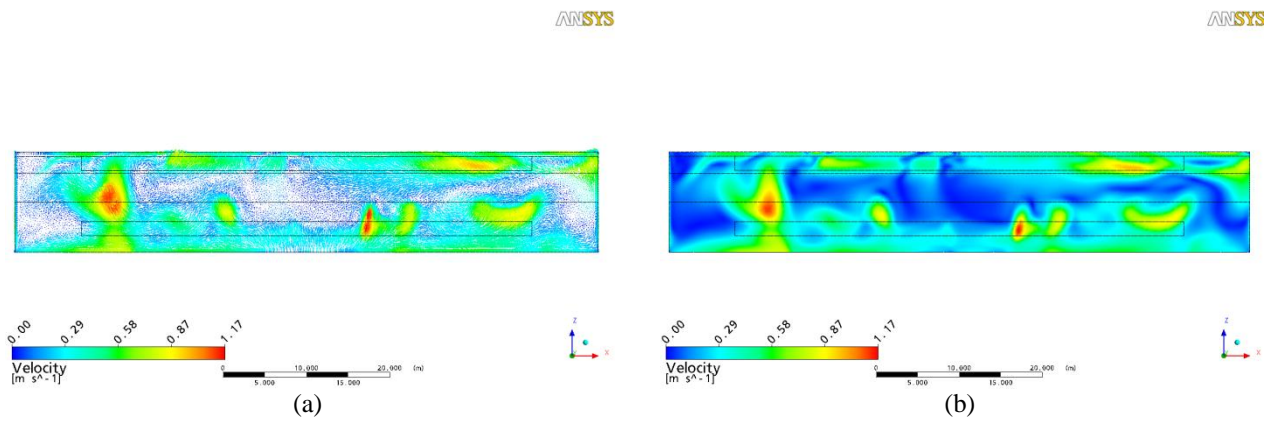


Figure 6. Velocity distribution on the region P4, velocity vectors (a) and velocity isosurfaces (b).

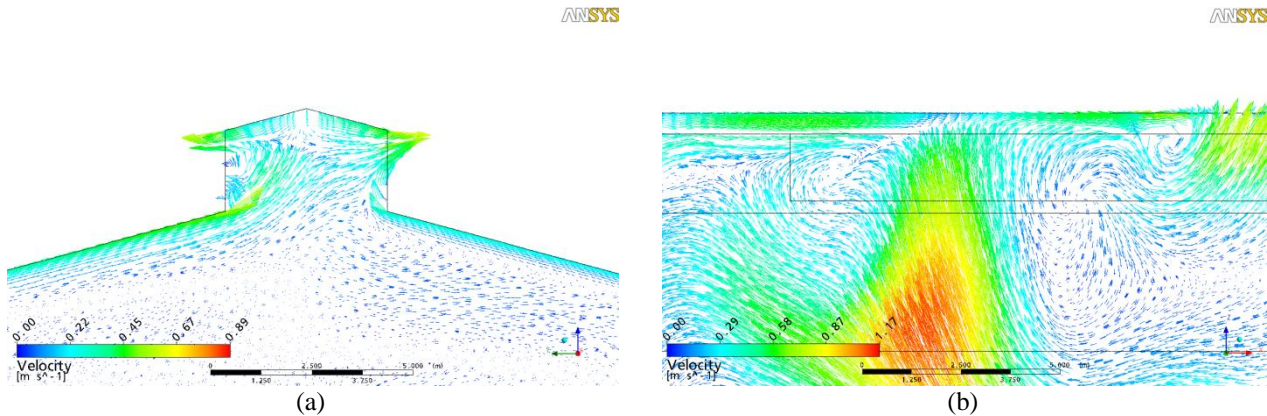


Figure 7. Velocity vectors in detail near the roof (a) and a hot source (b).

The result of simulation shows an average temperature inside the building is 313,15 K, presented as a  $\Delta t = 11 K$ . According to Macintyre (1990) the flow required to maintain this difference in temperature is shown in Eq. 18.

$$Q = \frac{C}{0,288 \cdot \Delta t} = \frac{2549851}{0,288 \cdot 11} = 804877 \text{ m}^3/\text{h} \quad (18)$$

According to the analytical model results obtained by numerical simulation was approximately 5 times less than the analytical results, thus showing high degree of conservatism of the model.

#### 4. CONCLUSIONS

The numeric model showed to be capable to represent the physics of the problem, where vertical displacements of masses of air due to the variation of density happened. Theoretical models for being too conservative, provide engineering projects extremely expensive. Like this with base in the present study, the methodology presented by Marcintyre (1990) showed a drainage approximately five times adult than calculated by the numeric model, that would end up providing larger equipments for removal and renewal of the mass of air contained in the building, generating like this a larger cost.

#### 5. REFERENCES

- CFX (2004). "CFX-10 Solver and Solver Manager Guide", AEA Technology Engineering Software Ltd, UK.
- Chow, W. K. (1996). "Application of Computational Fluid Dynamics in building services engineering." *Building and Environment* 31(5): 425-436.
- Costa, Ennio Cruz da (2005). "Ventilação", São Paulo: Edgard Blücher.
- Crouzeix, C., J. L. Le Mouël, et al. (2006). "Thermal stratification induced by heating in a non-adiabatic context." *Building and Environment* 41(7): 926-939.
- Gosselin, L. and Lacroix, M. (2003) "Heat transfer and banks formation in a slag bath with embedded heat sources.", *International Journal of Heat and Mass Transfer*, v.46, pp. 2537-2545.
- Incropera, F.P. and DeWitt, D.P. (2003) "Fundamentos de Transferência de Calor e Massa." Ed. LTC, 5ªed.
- Ji, Y., M. J. Cook, et al. (2007). "CFD modelling of natural displacement ventilation in an enclosure connected to an atrium." *Building and Environment* 42(3): 1158-1172.
- Kreith, F. e Bohn, M.S. (2003). "Princípios de Transferência de Calor." Ed. Thomson, 2ªed.
- Macintyre, A.J. (1990). "Ventilação industrial e controle da poluição." Ed. Guanabara, 2ªed.
- Mazon, A. A. O.; Silva, R. G. O.; Souza, H. A.; Ventilação natural em galpões: o uso de lanternins nas coberturas; REM: R. Esc. Minas, Ouro Preto, 59(2): 179-184, abr. jun. 2006184.
- Menter, F.R. (1993). "Multiscale model for turbulent flows", In 24th Fluid Dynamics Conference. American Institute of Aeronautics and Astronautics.
- Pirker, S., Gittler, P., Pirker, H. e Lehner, J. (2002). "CFD, a design tool for a new hot metal desulfurization technology." *Applied Mathematical Modelling*, v. 26, pp. 337-350.
- Seggiani, M. (1998). "Modelling and Simulation of time varying slag flow in a Prenfo entrained-flow gasifier." *Fuel*, v.77, n°14, pp. 1611-1621.
- Wilcox, D.C. (1986). "Multiscale model for turbulent flows", In AIAA 24th Aerospace Sciences Meeting. American Institute of Aeronautics and Astronautics.

## **6. RESPONSIBILITY NOTICE**

The author(s) is (are) the only responsible for the printed material included in this paper.